ISOLATING A LIGHT HIGGS BOSON FROM THE DI-PHOTON BACKGROUND AT THE LHC

Zvi Bern, Lance Dixon and Carl Schmidt
hep-ph-0206194

RADCOR 2002

Motivation

Why are we interested in the two-loop corrections to $gg \to \gamma\gamma$?

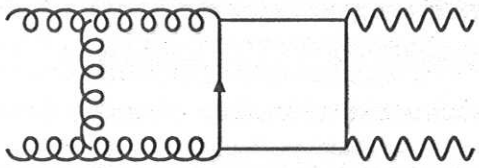

- If the Higgs is light ($M_H < 140$ GeV) difficult to extract the Higgs signal from the di-photon background. Reliable theoretical calculations can help us find better search strategies.

- Considerable effort has gone into developing methods for computing two-loop corrections to $2 \to 2$ scattering. It is helpful to have examples demonstrating a definite impact on phenomenology.

Where is the Higgs Boson?

Under the assumption of a Standard Model Higgs, virtual loop corrections pin down the Higgs mass.

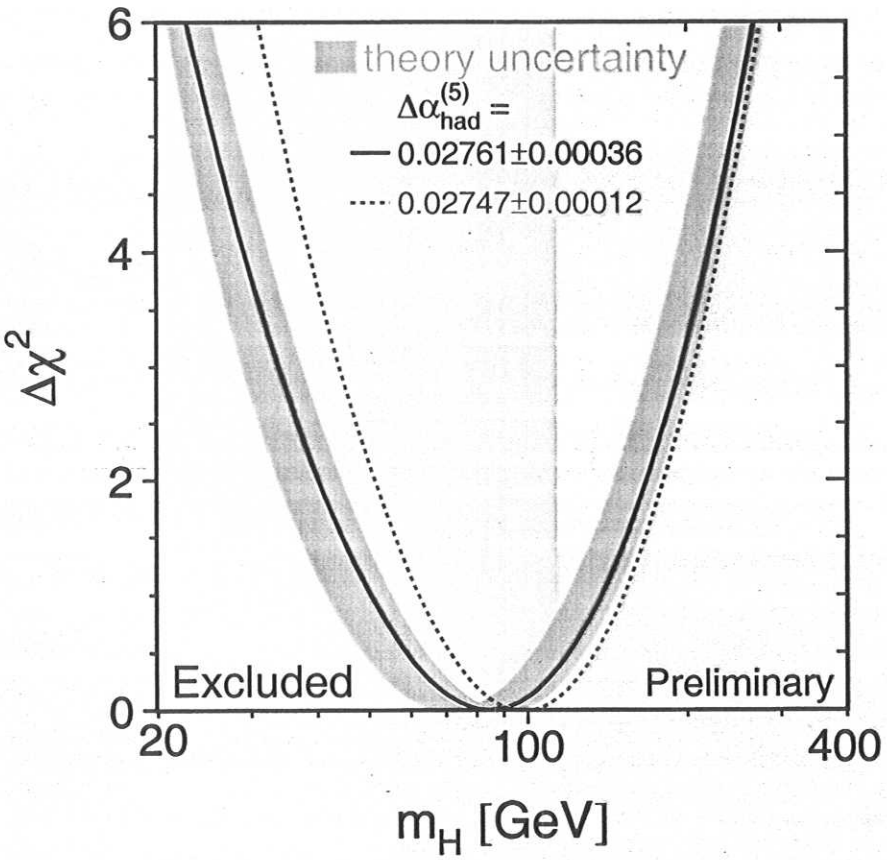

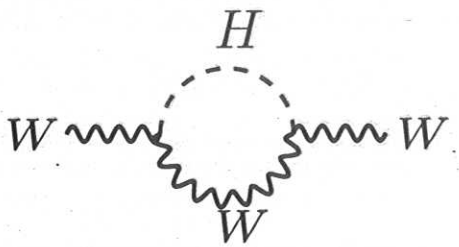

$m_H < 196$ GeV at 95% confidence level.

LEP found a hint of the Higgs at the end point of its energy reach: $M_H = 115$ GeV.

Higgs Boson Search at the LHC

Higgs discovery potential at the LHC

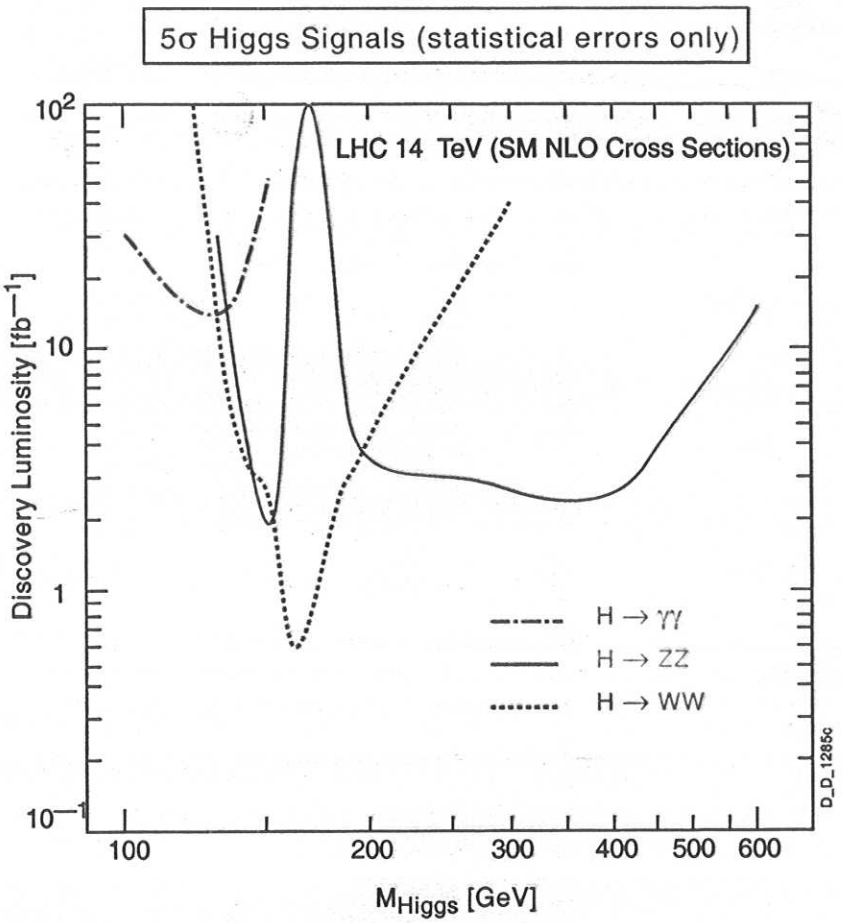

The LHC at startup should achieve 10 fb^{-1}/year.

For $M_H < 140$ GeV di-photon channel is the best option.

$H_{SM} \rightarrow \gamma\gamma$

Simulated 2γ mass plot
for 10^5 pb^{-1} m_H =130 GeV
in the lead tungstate calorimeter

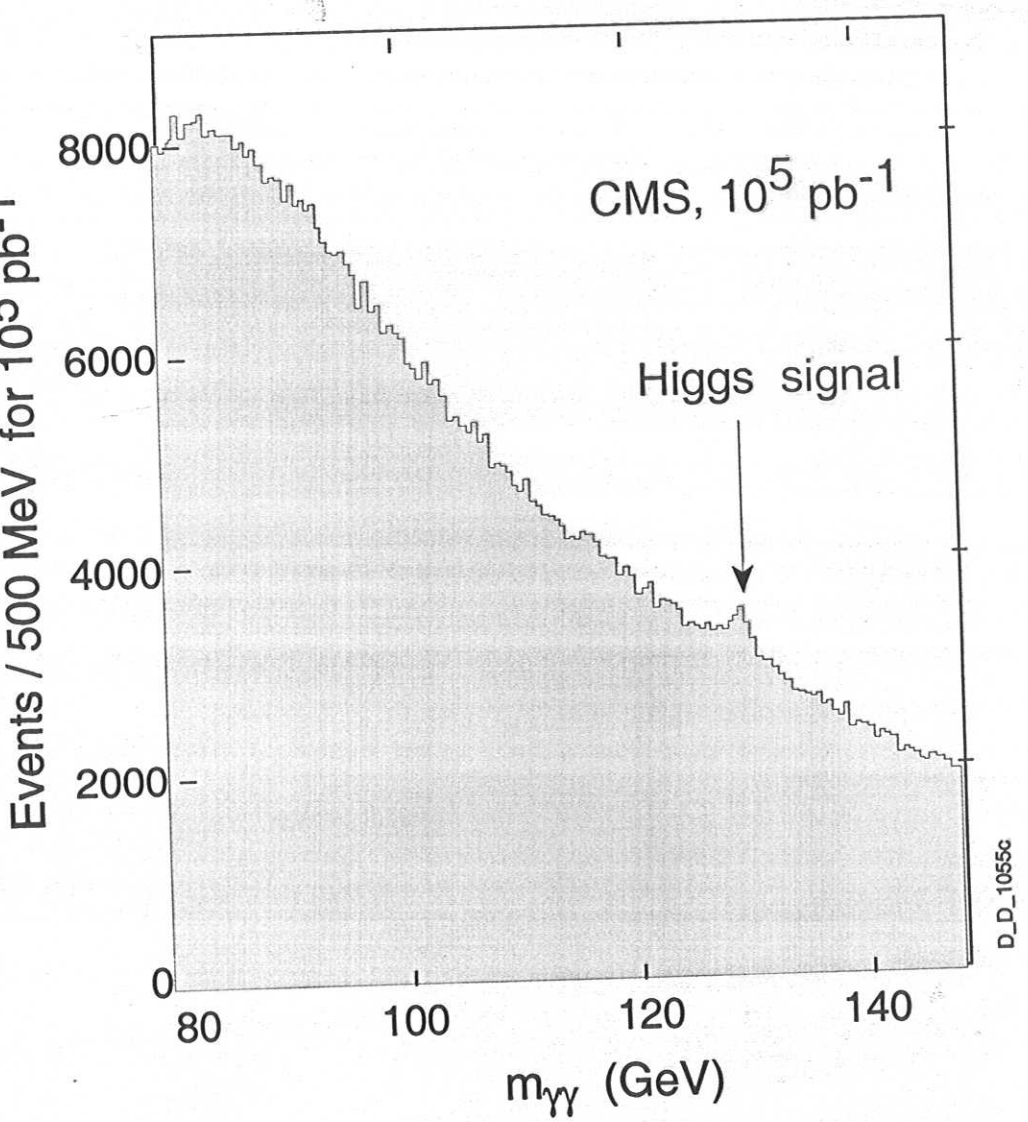

Note that this is for 100 fb^{-1}

Here we focus on QCD background.

DIPHOX

NLO corrections to the $q\bar{q} \to \gamma\gamma$ QCD background subprocess have been computed by a number of groups.

E.L. Berger, E. Braaten and R.D. Field; Aurenche, Douiri, Baier, Fontannaz, Schiff; Bailey, Graudenz, Owens, Ohnemus; Balazs, Berger, Mrenna, Yuan; Binoth, Guillet, Pilon, Werlen

Prompt photons produced not only directly in hard processes, but also by fragmentation of quarks and gluons.

All of the above are incorporated at NLO in a flexible program: DIPHOX

Binoth, Guillet, Pilon, Werlen

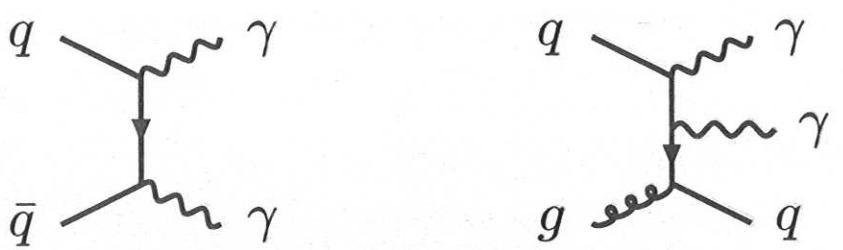

The largest NLO contribution missing from DIPHOX are for gluon fusion which is incorporated only at LO.

We use DIPHOX for all but the $gg \to \gamma\gamma$ contributions.

Photon Isolation

To reduce fragmentation contribution, and also reject jets or π^0s faking photon isolation criteria are imposed.

Two choices: $\eta = \ln \tan(\theta/2)$.

1. Standard Cone isolation — the amount of transverse hadronic energy $E_{\rm T}$ in a cone of radius $R = \sqrt{(\Delta\eta)^2 + (\Delta\phi)^2}$ must be less than $E_{\rm T\,max}$.

2. Smooth (Frixione) Cone Isolation — the amount of transverse hadronic energy $E_{\rm T}$ in *all* cones of radius r with $r < R$ must be less than (Not in DIPHOX)

$$E_{\rm T\,max}(r) \equiv p_{\rm T}(\gamma)\,\epsilon \left(\frac{1-\cos r}{1-\cos R}\right)$$

Theoretically the smooth cone algorithm is preferred because it completely suppresses fragmentation contribution. But it may be difficult to exploit experimentally (transverse shower extent, finite detector granularity).

Gluon Fusion Background to $H \to \gamma\gamma$

For a low mass Higgs ($M_H < 140$ GeV) the preferred search mode is via the rare decay $H \to \gamma\gamma$.

LHC is a glue factory, hence gluon fusion is important background:

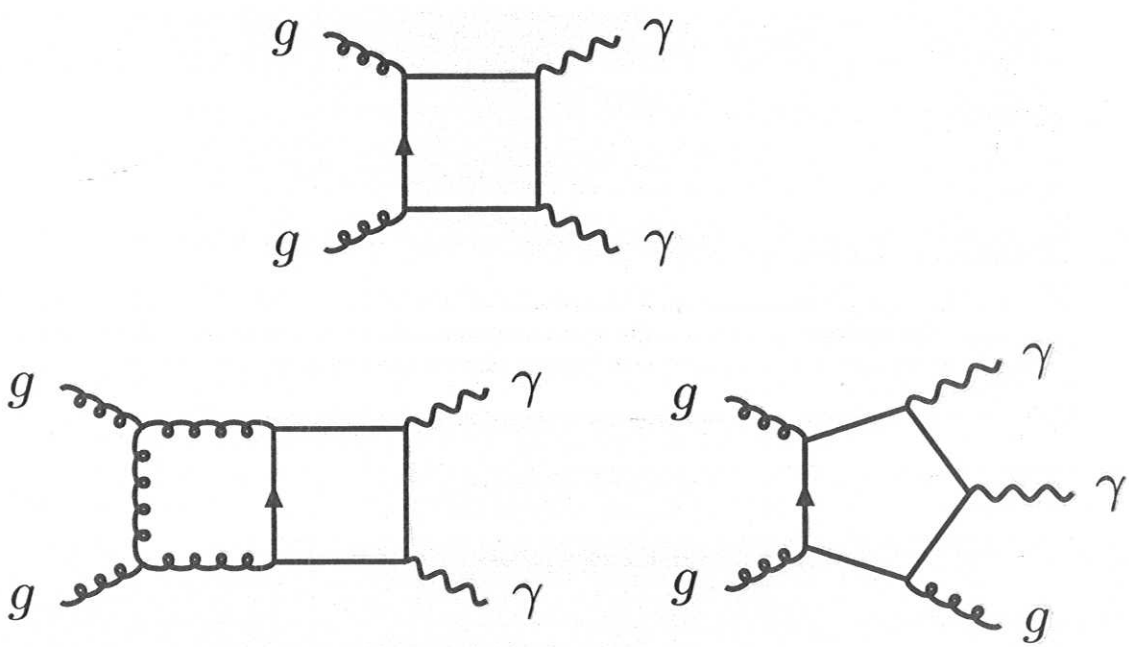

NLO corrections to gluon fusion are sizable.

Note: this is N^3LO with respect to entire process.

Real Emission Contributions

The one-loop 5 gluon amplitudes were calculated in 1993.

ZB, Dixon, Kosower

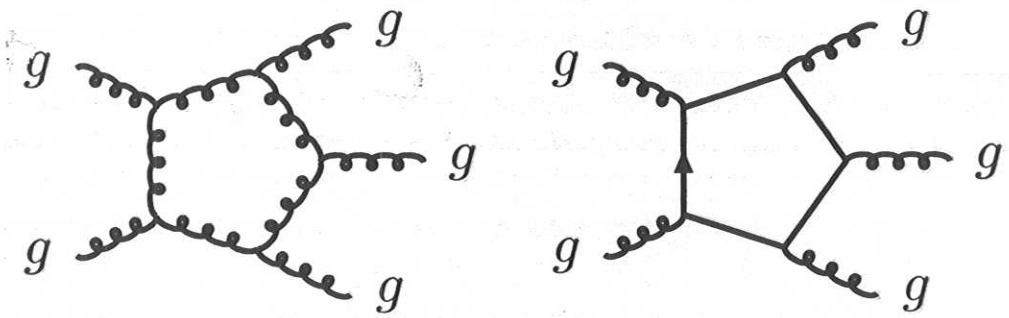

The $gg \to \gamma\gamma g$ amplitudes are obtained from the quark loop amplitudes by summing appropriate permutations:

de Florian, Kunszt; Balazs, Nadolsky, Schmidt, Yuan

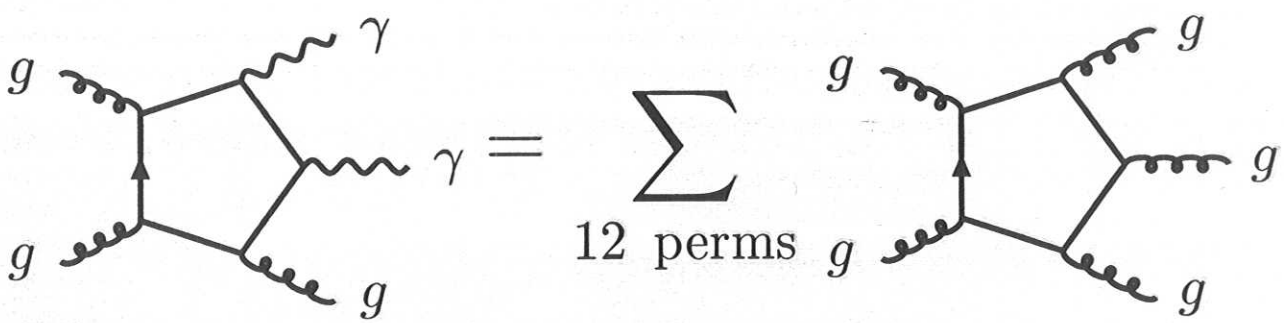

No IR or UV divergences in amplitude since tree process vanishes in the one-loop $g \to \gamma\gamma g$ amplitude.

Virtual Contributions

Z.B, De Freitas, Dixon

The calculation of the virtual contributions were already described in Abilio De Freitas' talk.

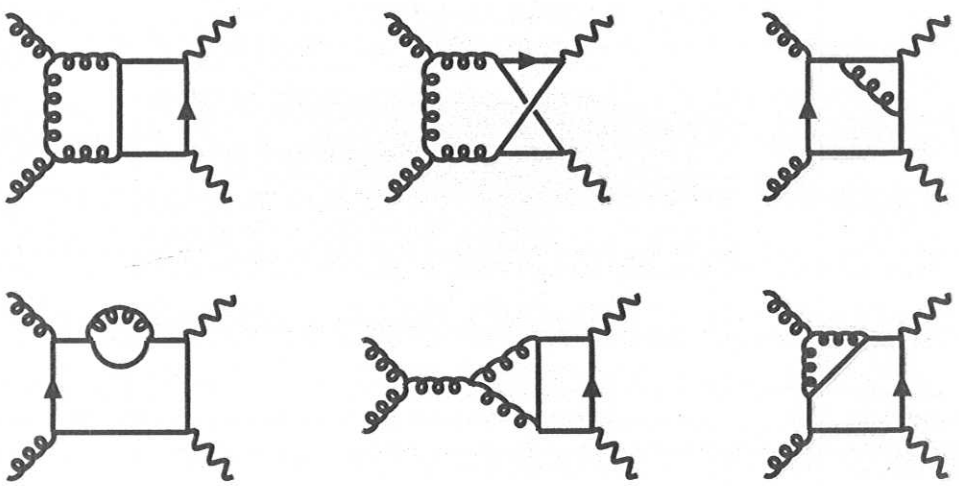

Two-loop Infrared Divergences

Catani, hep-ph/9802439

Stefano Catani has provided us with a general formula for two-loop IR divergences in QCD.

IR structure of 2-loop $gg \to \gamma\gamma$ amplitude is simple (tree vanishes):

$$\mathcal{M}^{\text{2-loop}}_{gg\to\gamma\gamma} = \frac{2\alpha\,\alpha_s^2(\mu)}{\pi}\delta^{a_1a_2}\left(\sum_i Q_i^2\right)\Bigg\{ \left[\boldsymbol{I}^{(1)}(\epsilon) + \frac{11N - 2N_f}{6}\left(\ln(\mu^2/s) + i\pi\right)\right] M^{(1)} + NF^{\mathrm{L}}(s,t) - \frac{1}{N}F^{\mathrm{SL}}(s,t)\Bigg\}$$

where

$$\boldsymbol{I}^{(1)}(\epsilon) = -N\frac{e^{-\epsilon\psi(1)}}{\Gamma(1-\epsilon)}\left[\frac{1}{\epsilon^2} + \left(\frac{11}{6} - \frac{1}{3}\frac{N_f}{N}\right)\frac{1}{\epsilon}\right]\left(\frac{\mu^2}{-s}\right)^{\epsilon}$$

$$\mathcal{M}^{\text{1-loop}}_{gg\to\gamma\gamma} = 4\alpha\,\alpha_s(\mu)\delta^{a_1a_2}\left(\sum_i Q_i^2\right) M^{(1)}$$

Sample Two-Loop Finite Parts for $gg \to \gamma\gamma$

Z.B, De Freitas, Dixon

where

$$
\begin{aligned}
M^{(2)}_{--++} &= -\frac{3}{2}, \\
M^{(2)}_{-+++} &= \frac{1}{8}\Big[\Big(\frac{x^4}{y^2}+\frac{1}{y^2}-2\frac{x^2}{y}+y^2\Big)X^2-\frac{1}{2}(x^2+y^2)(2XY-\pi^2)-4\Big(\frac{x^2}{y}-1\Big)X \\
&\qquad +2i\pi\Big[\Big(1-2\frac{x}{y^2}\Big)X+\frac{x}{y}-\frac{1}{x}\Big]\Big] \;+\; \{t\leftrightarrow u\}, \\
M^{(2)}_{++++} &= -2(x^2+y^2)\mathrm{Li}_4(-x)-(x-y)\mathrm{Li}_4(-x/y)+2x^2X\Big(\mathrm{Li}_3(-x)+\mathrm{Li}_3(-y)\Big) \\
&\quad +\frac{\pi^2}{6}(x-y)\mathrm{Li}_2(-x)+x^2\Big(-\frac{1}{6}X^4+\frac{2}{3}X^3Y-\frac{\pi^2}{6}XY+\frac{4}{45}\pi^4\Big) \\
&\quad -(3x+y)\Big(\mathrm{Li}_3(-x)-X\mathrm{Li}_2(-x)\Big)-\frac{1}{12}(9x-y)(X^3-3X^2Y) \\
&\quad +(3x+5y)\frac{\pi^2}{12}X-2\zeta_3-\frac{1}{4}\Big(\frac{x^4}{y^2}-x^2+4xy+2y^2\Big)X^2+\frac{1}{2}(3x+4y)xXY \\
&\quad -(7x+10y)x\frac{\pi^2}{12}+\frac{1}{2}\Big(\frac{x^2}{y}+4x+y\Big)X-\frac{1}{4} \\
&\quad +i\pi\Big[2(x^2+y^2)\mathrm{Li}_3(-x)-x^2\Big(\frac{1}{3}X(X^2+\pi^2)-X^2Y\Big) \\
&\qquad +\frac{1}{2}(x-y)\Big(\mathrm{Li}_2(-x)-\mathrm{Li}_2(-y)\Big)-\frac{1}{2}(3x+y)X^2+2x\Big(XY-\frac{\pi^2}{6}\Big) \\
&\qquad +\frac{1}{2}\Big(-\frac{x^2}{y^2}+2\frac{x}{y}+1\Big)X-\frac{x}{2y}-1\Big] \;+\; \{t\leftrightarrow u\}, \\
M^{(2)}_{+--+} &= 2\Big(2\frac{x}{y^2}-1\Big)\Big(\mathrm{Li}_4(-x/y)-\mathrm{Li}_4(-y)-Y(\mathrm{Li}_3(-x)-\zeta_3) \\
&\qquad +\frac{1}{48}X^4-\frac{1}{6}XY^3+\frac{1}{24}Y^4+\frac{\pi^2}{12}Y^2-\frac{7}{360}\pi^4\Big) \\
&\quad -2\Big(2\frac{x}{y}+1\Big)\Big(\mathrm{Li}_4(-x)+\frac{\pi^2}{6}\mathrm{Li}_2(-x)-\frac{\pi^2}{12}X^2\Big)-2\frac{x^2}{y^2}\Big(X(\mathrm{Li}_3(-x)-\zeta_3)+\frac{1}{24}X^4+\frac{7}{90}\pi^4\Big) \\
&\quad +\Big(2\frac{x}{y}-1\Big)\Big(\mathrm{Li}_3(-x)-X\mathrm{Li}_2(-x)-\frac{\pi^2}{3}Y\Big)+2\Big(2\frac{x}{y}+1\Big)\Big(\mathrm{Li}_3(-y)+Y\mathrm{Li}_2(-x)+\frac{1}{2}XY^2\Big) \\
&\quad -\frac{1}{12}\Big(10\frac{x}{y}+1\Big)X^3+\frac{\pi^2}{6}\Big(2\frac{x}{y}+5\Big)X-\Big(2\frac{x}{y}+3\Big)\zeta_3+\frac{1}{4}\Big(2\frac{x^4}{y^2}+6\frac{x^3}{y}+x^2-4xy-2y^2\Big)X^2 \\
&\quad +\frac{1}{2}(2x^2-y^2)XY-\frac{1}{4}\Big(4x^2+8xy+10y^2+6\frac{y^3}{x}+\frac{y^4}{x^2}\Big)Y^2-(4x^2-4xy-5y^2)\frac{\pi^2}{12} \\
&\quad +\frac{1}{2}(2x+y^2)\Big(\frac{X}{y}+\frac{Y}{x}\Big)-\frac{1}{2} \\
&\quad +i\pi\Big[\frac{2}{y^2}(\mathrm{Li}_3(-x)-\zeta_3)+\frac{1}{6}\Big(2\frac{x}{y^2}-1\Big)X^3+\Big(2\frac{x}{y}+3\Big)\mathrm{Li}_2(-x)-\frac{3}{4}\Big(2\frac{x}{y}+1\Big)X^2 \\
&\qquad -\frac{1}{2}\Big(2\frac{x}{y^2}+3\Big)X-\frac{1}{2}\Big(2+4\frac{y}{x}+\frac{y^2}{x^2}\Big)Y-\frac{1}{y}-\frac{y}{2x}\Big].
\end{aligned}
\tag{2.7}
$$

Here

$$
x\equiv\frac{t}{s},\quad y\equiv\frac{u}{s},\quad X\equiv\ln\Big(-\frac{t}{s}\Big),\quad Y\equiv\ln\Big(-\frac{u}{s}\Big). \tag{2.8}
$$

Subleading color piece

Phase Space Integration

To obtain a physical cross-section the two-loop $gg \to \gamma\gamma$ amplitude must be combined with the one-loop real emission diagrams.

Integral over final gluon phase space diverges when gluon is soft, or collinear with an initial gluon. Similar to typical QCD NLO computations.

To deal with this we applied the dipole method of Catani and Seymour.

Phase-space integral of dipole terms gives poles in $\epsilon = (4 - D)/2$. which cancel poles from 2-loop amplitude, up to the collinear counterterm for initial state factorization.

Subtracted integral is finite, so integrals can be done numerically in $D = 4$.

Omitted contributions to $pp \to \gamma\gamma X$

Contributions at $\mathcal{O}(\alpha_s^2)$ which are still omitted:

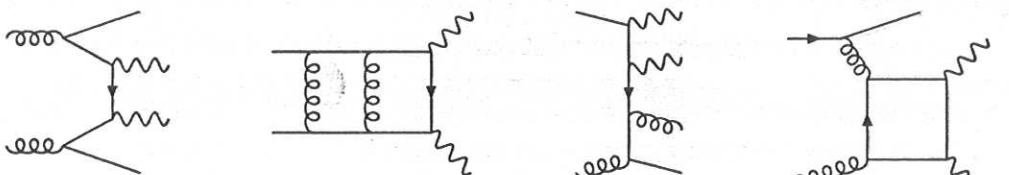

(a) Recent $gg \to W\gamma q\bar{q}'$ calculation of Adamson, de Florian, Signer suggests it is small.

(b) Calculated by Anastasiou, Glover, Tejeda-Yeomans [redacted] but need to handle double real radiation

(c) Double real radiation. The qg initiated subprocesses may be more tractable than $q\bar{q}$ initiated process.

(d) likely to be small since it lacks both initial and final state singularities.

The gg fusion contributions described in this talk were the largest missing pieces. It would be also be important to calculate the other missing pieces to verify that there are no surprises.

Phenomenological Implications of NLO

$gg \to \gamma\gamma$

Binoth, Guillet, Pilon, Werlen

Z.B., Dixon and Schmidt

Shift due to including the NLO $gg \to \gamma\gamma$

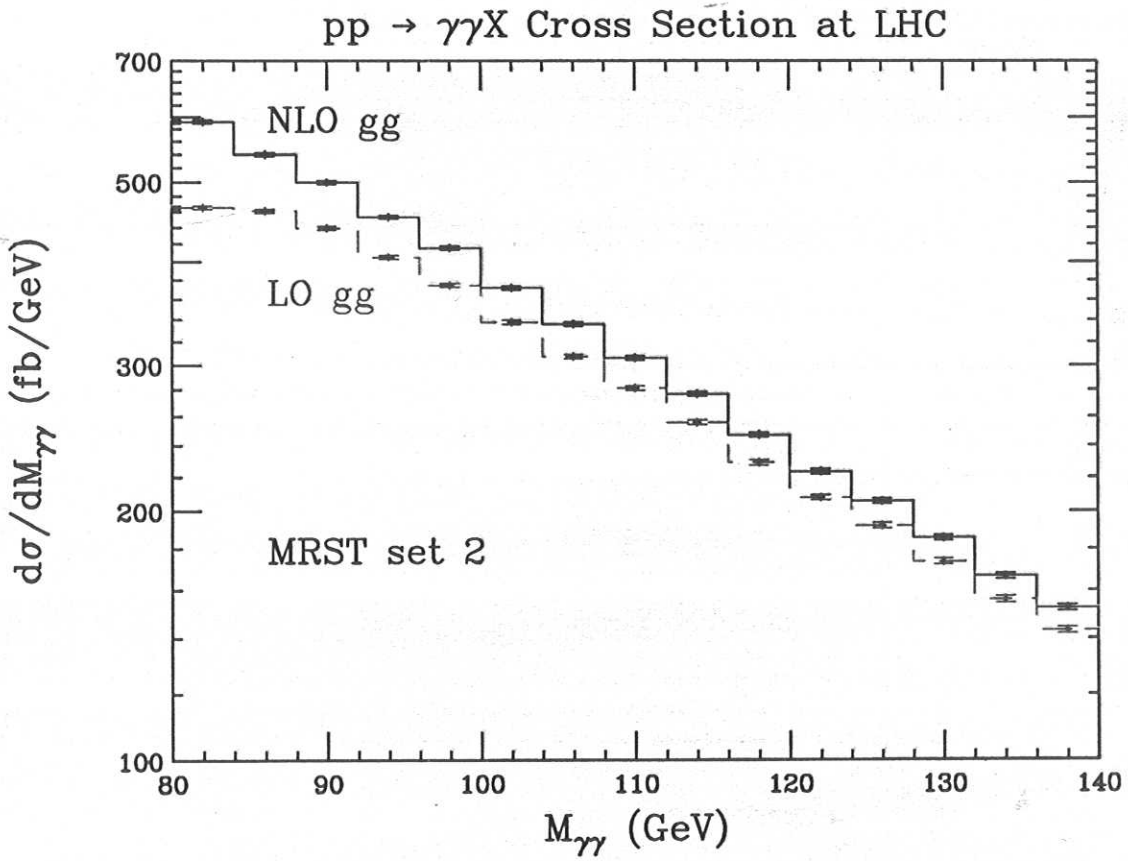

K Factors

Previously K factor of $gg \to \gamma\gamma$ was estimated using known K factor of $gg \to H$.

However, as our explicit calculation shows they are quite different.

Comparison of NLO QCD K factors (ratio of NLO to LO cross-sections):

$M_{\gamma\gamma}$ (GeV)	K_{Higgs}	$K_{gg\to\gamma\gamma}$
98	2.92	1.82
118	2.54	1.61
138	2.39	1.55

Same kinematic cuts, $\mu_R = \mu_F = 0.5\, M_{\gamma\gamma}$.
(K factors here defined using NLO pdfs to compute LO cross section which gives larger K factors than the standard ones.)

K factors significantly smaller than obtained from previous estimate.

Diagonal Scale Variation, $\mu_R = \mu_F$

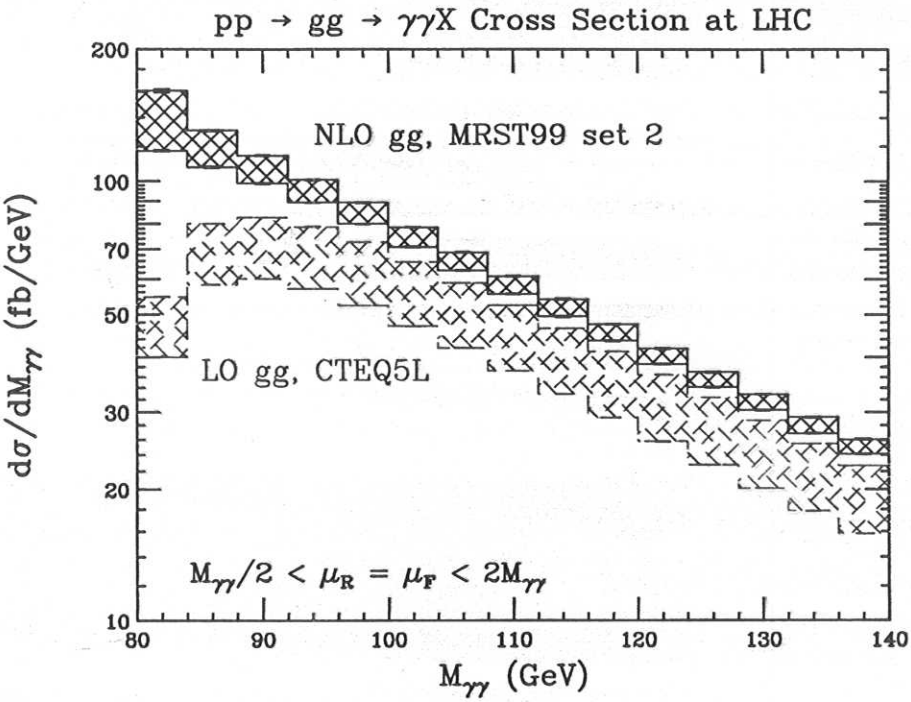

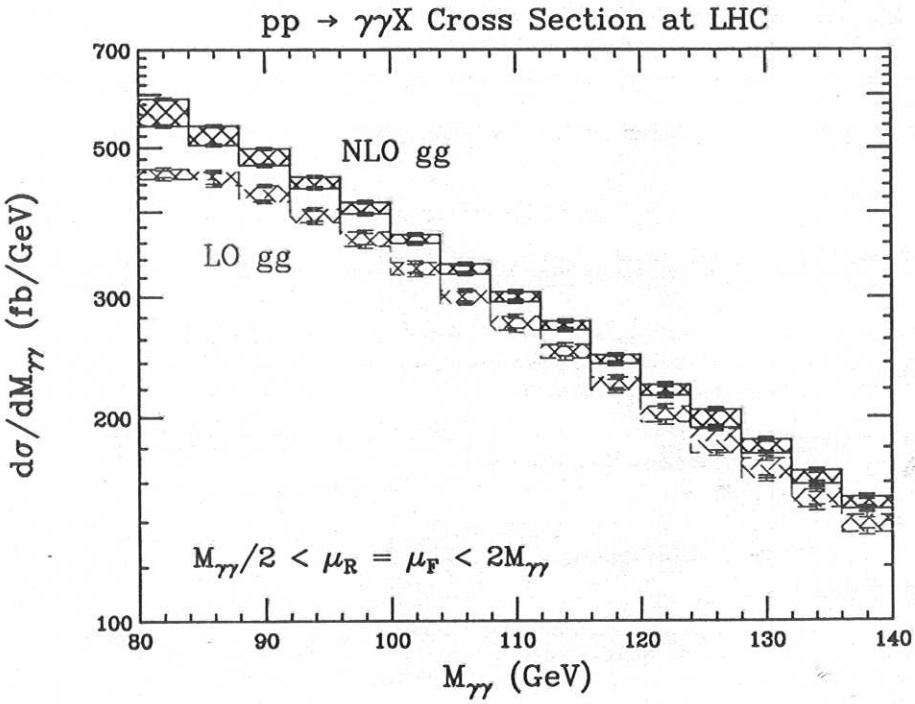

Scale Variation

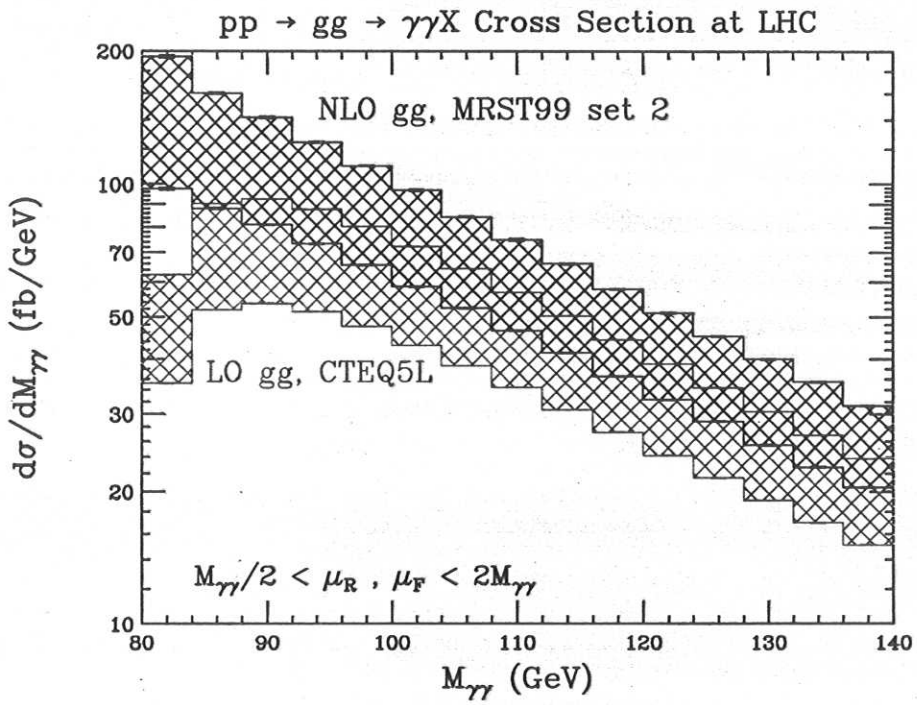

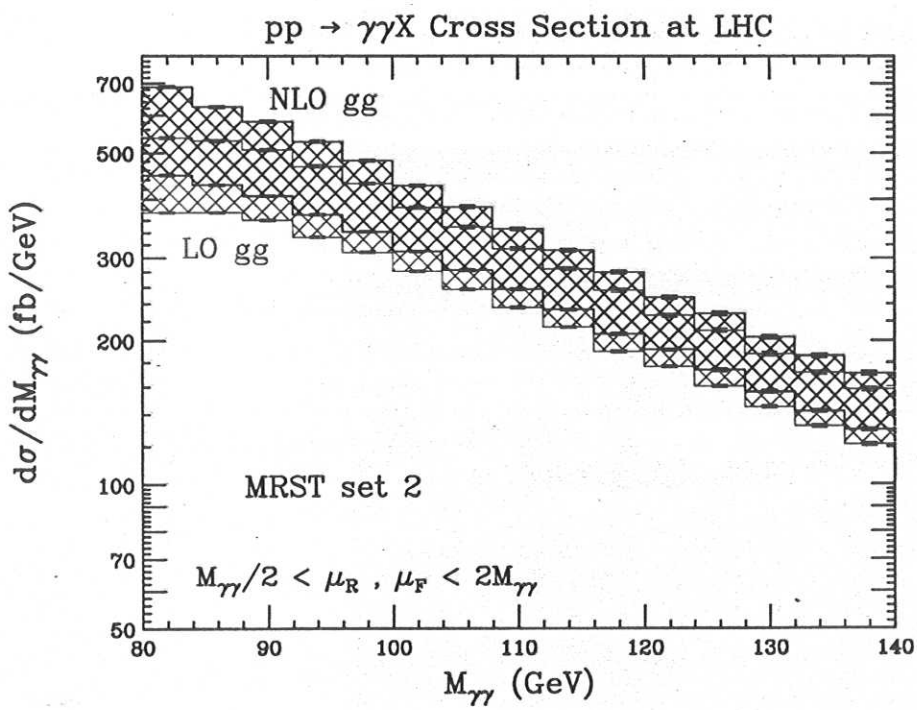

PDF dependence

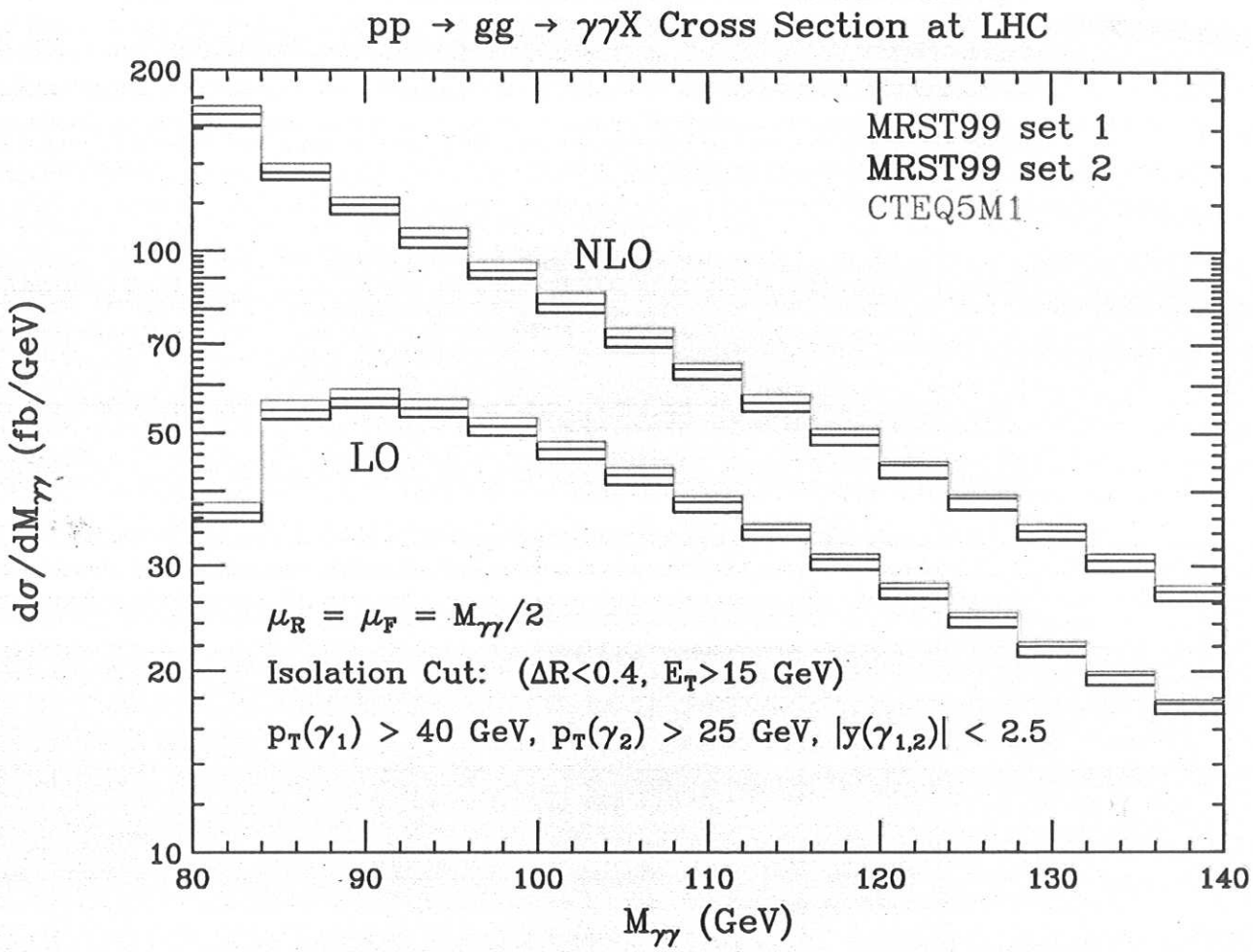

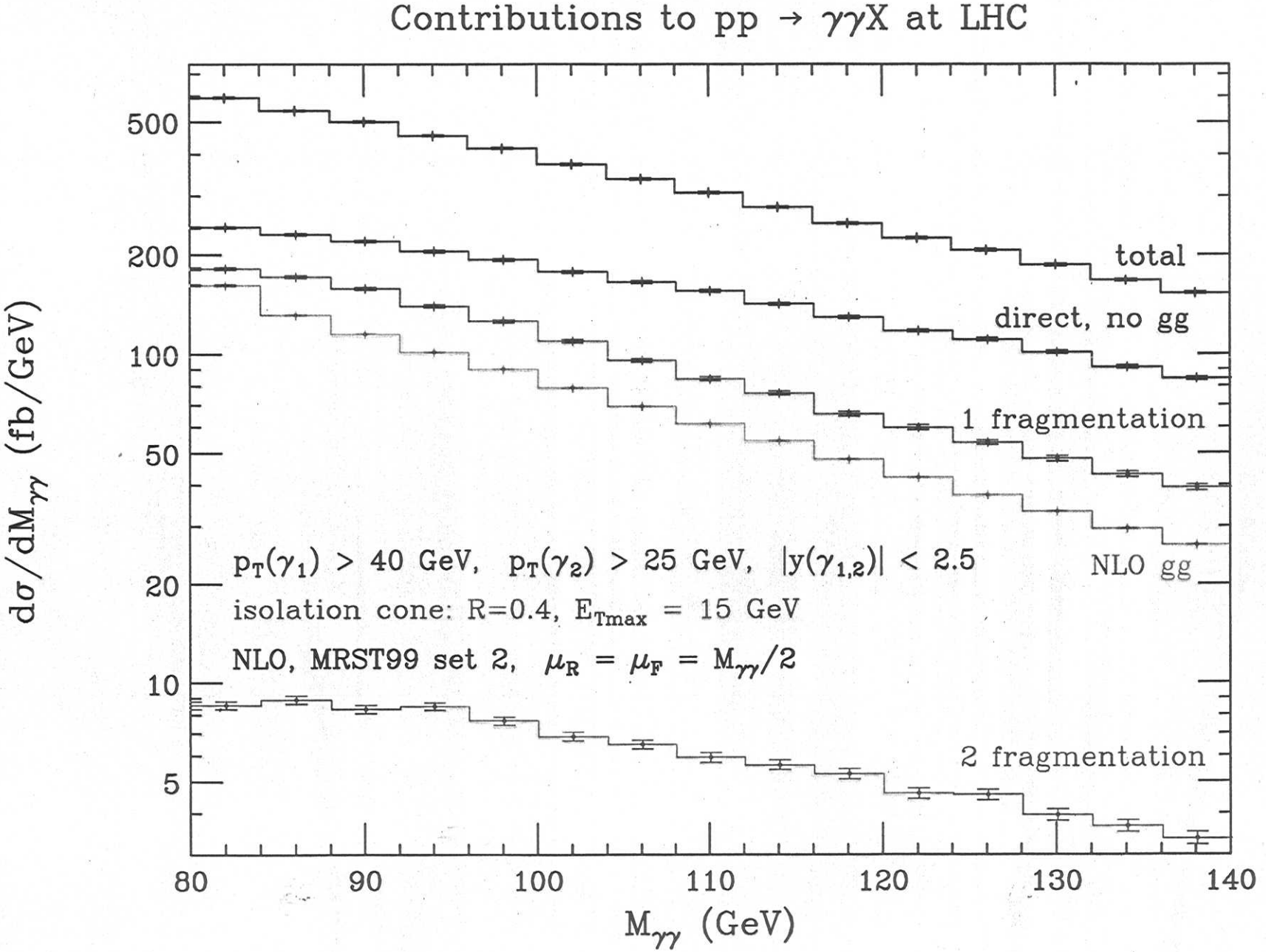
Contributions to pp → γγX at LHC
dσ/dM$_{γγ}$ (fb/GeV)
M$_{γγ}$ (GeV)
500
200
100
50
20
10
5
80
90
100
110
120
130
140
total
direct, no gg
1 fragmentation
NLO gg
2 fragmentation
p$_T$(γ$_1$) > 40 GeV, p$_T$(γ$_2$) > 25 GeV, |y(γ$_{1,2}$)| < 2.5
isolation cone: R=0.4, E$_{Tmax}$ = 15 GeV
NLO, MRST99 set 2, μ$_R$ = μ$_F$ = M$_{γγ}$/2

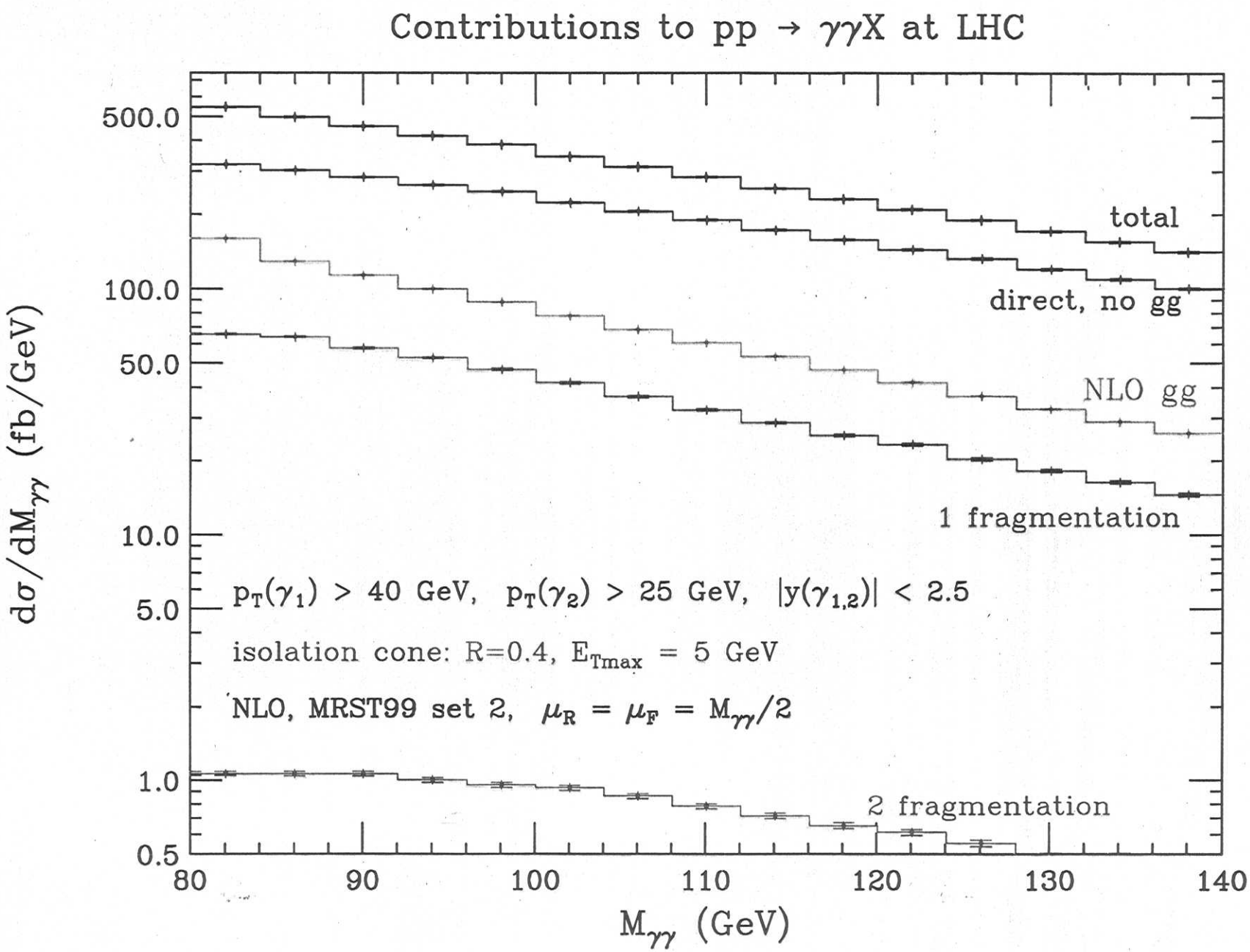
Contributions to pp → γγX at LHC
500.0
100.0
50.0
10.0
5.0
1.0
0.5
80
90
100
110
120
130
140
dσ/dM_γγ (fb/GeV)
M_γγ (GeV)
total
direct, no gg
NLO gg
1 fragmentation
2 fragmentation
p_T(γ_1) > 40 GeV, p_T(γ_2) > 25 GeV, |y(γ_1,2)| < 2.5
isolation cone: R=0.4, E_Tmax = 5 GeV
NLO, MRST99 set 2, μ_R = μ_F = M_γγ/2

The Higgs signal at the LHC

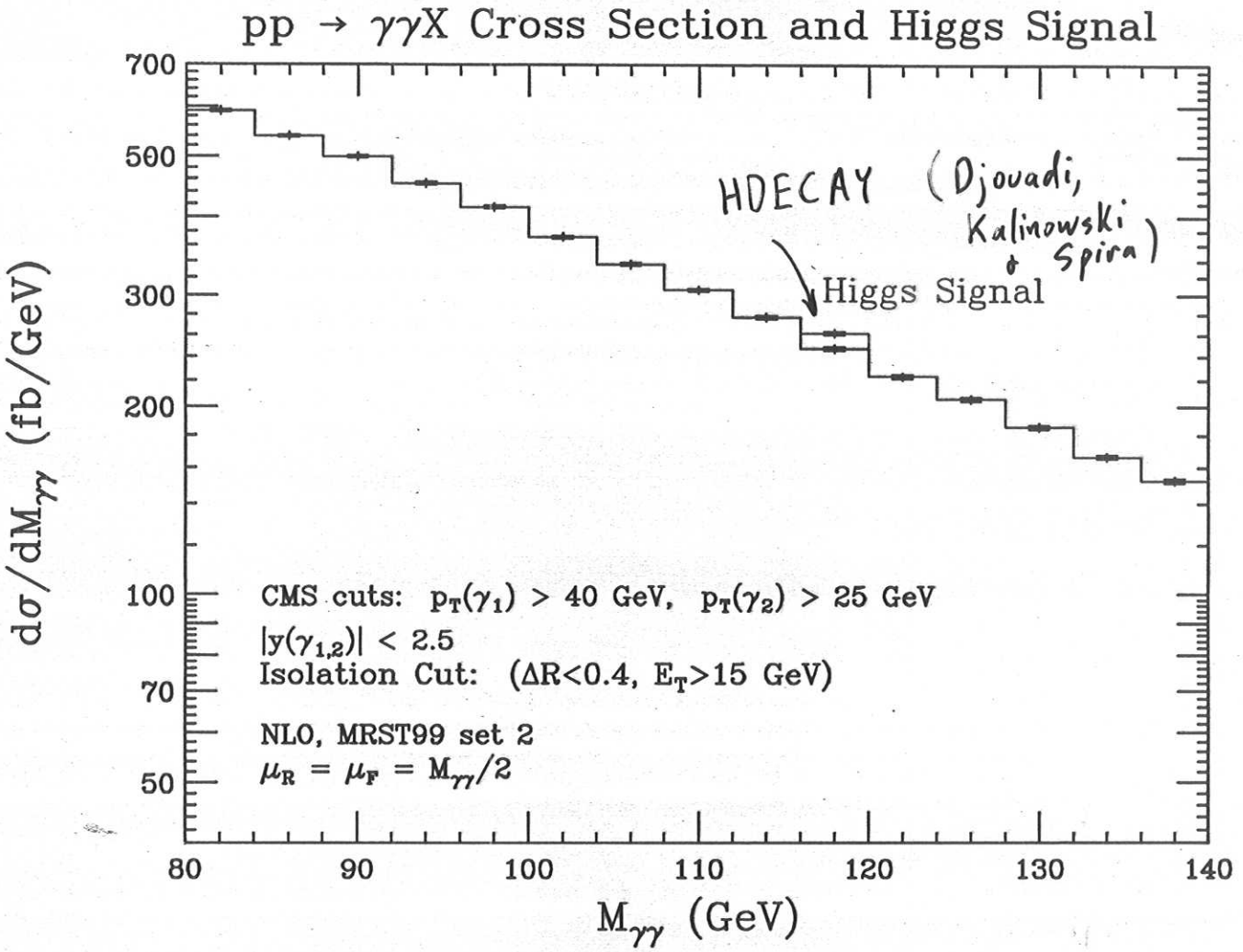

It will take about 2 years of running to pull the signal out of the background. Can we improve the situation?

Interference Between S & B

Naively there are huge interfence effects:

$$(\sqrt{S} + \sqrt{B})^2 = B + 2\sqrt{S}\sqrt{B} + S$$

$S << B$

↑ seems large

However, this is <u>not</u> how it works.

If we had a detector that can resolve Higgs resonance

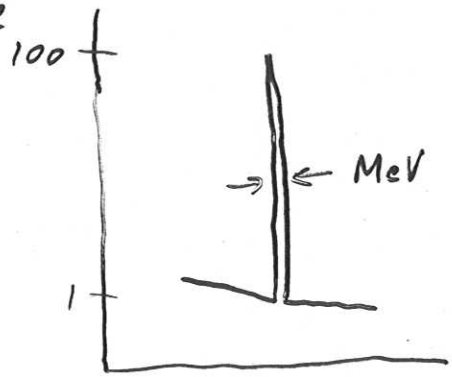

$$(\sqrt{S} + \sqrt{B})^2 = 1 + 20 + 100$$

↑ B ↑ $2\sqrt{S}\sqrt{B}$ ↑ S

$\Rightarrow$ 20% effect.

This still might be important.

However there are a few other effects that reduces it even further.

Spin 0 Higgs decays into identical helicity photons

Interference term is: (integrates to zero.)

$$2\,\mathrm{Re}\left[A^*(gg\to H)\,\frac{(s-m_H^2)-i\Gamma_H m_H}{(s-m_H)^2+\Gamma_H^2 m_H^2}\,A^*(H\to\gamma^+\gamma^+)\times A^{\text{Background}}(gg\to\gamma^+\gamma^+)\right]$$

However at LO amplitudes are all real.

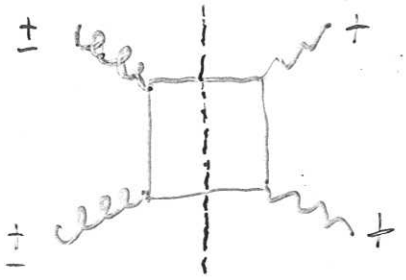

← No Imaginary part.
(can prove via susy Ward Id.)
(hep-ph/0109078)

$s-m_H^2$ term integrates to zero.
$i\Gamma_H m_H$ vanishes because of "Re"

⇒ Interference is only an NLO effect.
Extra α_s.

⇒ Expect ~ 1% effect.
Verified by explicit calculation.

Interference is very small

Angular distribution

Higgs decay is isotropic.

QCD background is not isotropic

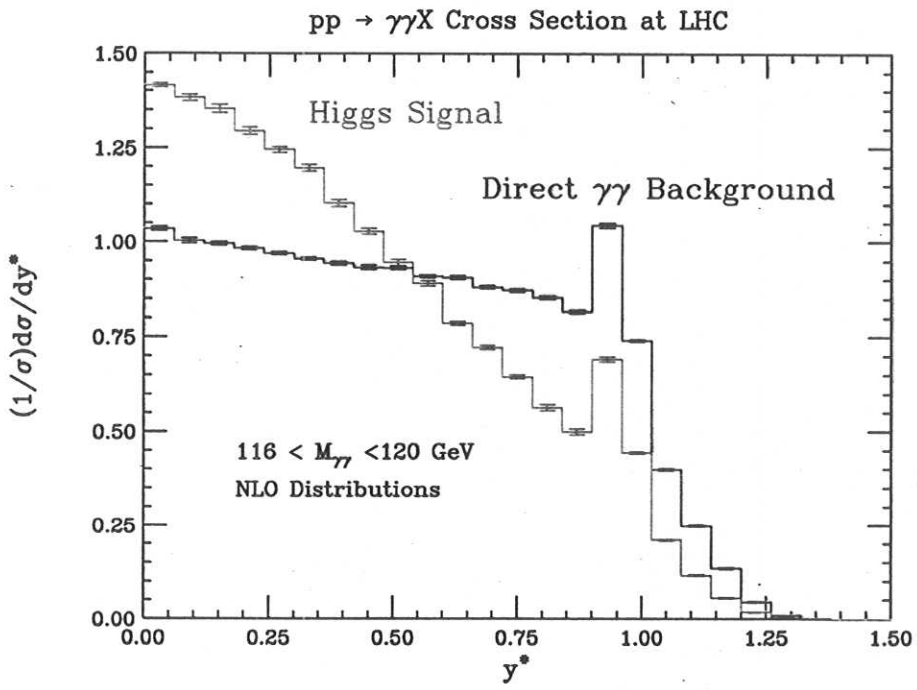

y^* is rapidity difference $\frac{1}{2}(y(\gamma_1) - y(\gamma_2))$

smooth cone, $R = 1$, $\epsilon = 1$.

The peaks at $y^* = 0.94$ are artifacts of the NLO calculation which happen at kinematic boundaries of LO calculation coming from the cut $p_T(\gamma_1) > 40$ GeV. Need to resum large logs.

Berger and Qiu; Catani, Fontannaz and Pilon; Binoth, Guillet, Pilon and Werlen

Dependence on Photon Isolation Cone

V. Tissarand
T. Binoth, J.P. Guillet, E. Pilon, M. Werlen
Z.B., Dixon and Schmidt

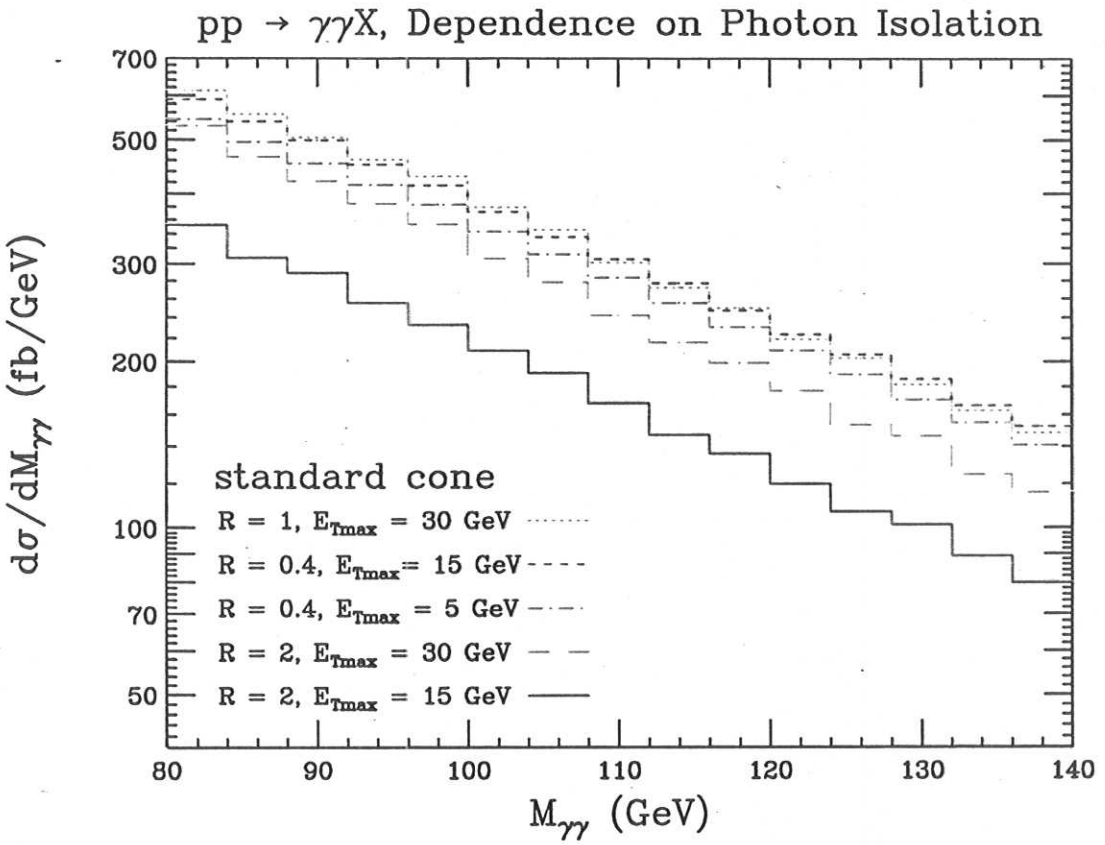

By studying different ways of isolating the photon from hadronic energy it should be possible to optimize $S/\sqrt{B}$.

To really understand what is happening a more realistic simulation is needed, including detector effects, π_0 background, etc.

Using a jet veto is an experimentally preferred way to reject background with nearby hadronic energy.

Effect of Jet Veto

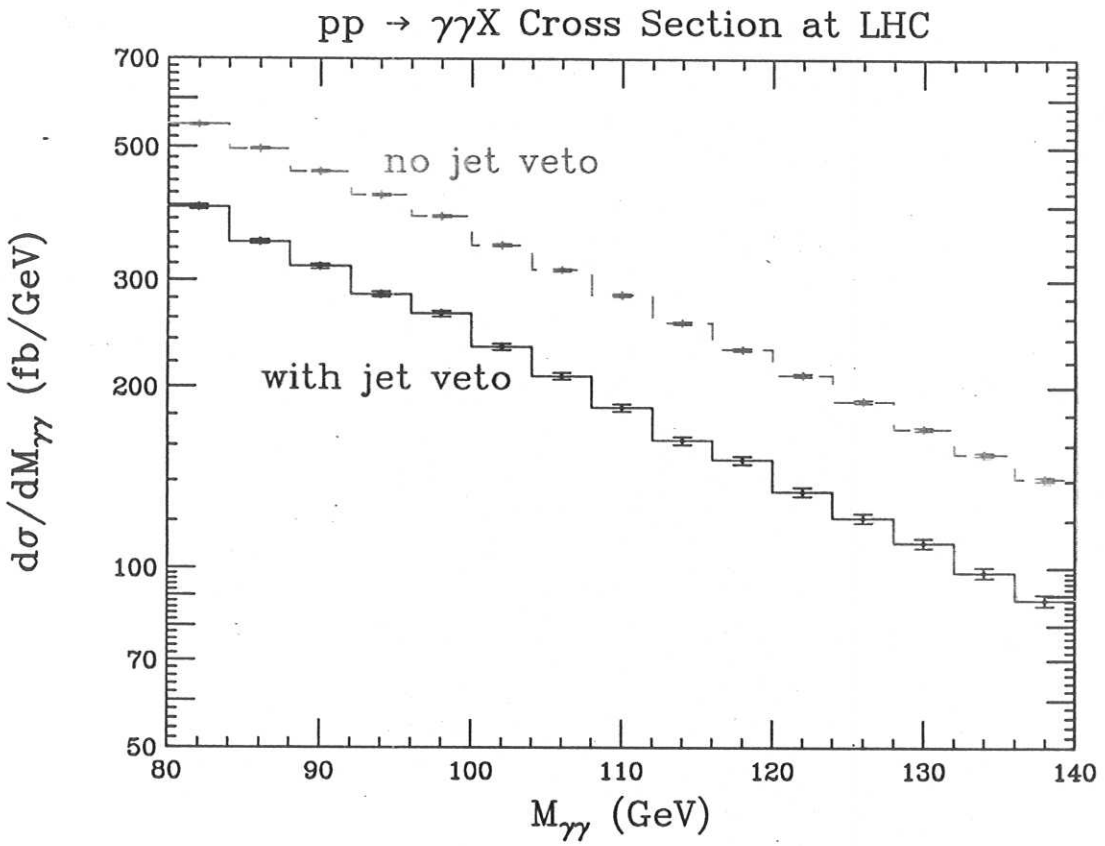

Veto on jets with $E_T > 15$ GeV within $R_{\text{jet}} = 2$.

Veto is on top of the standard isolation cone with $R = 0.4$ and $E_{\text{T max}} = 5GeV$.

Unfortunately, the Higgs signal is also reduced so statistical significance is essentially unchanged!

Summary

1. NLO $gg \to \gamma\gamma$ was the first application of the new two loop QCD amplitudes to phenomenology. More studies will be forthcoming.

2. QCD corrections to the gluon fusion subprocess, $pp \to gg \to \gamma\gamma X$ are under adequate control. The K factor for this subprocess is significantly smaller than that for Higgs production, $pp \to gg \to HX$.

3. Reliable theoretical calculations may help us find improved ways to enhance the Higgs signal compared to the background.